Energy transfer dynamics of dissipative trapped ion convective cell turbulence

D. E. Newman and P. W. Terry
Department of Physics, University of Wisconsin—Madison, Madison, Wisconsin 53706

P. H. Diamond
Department of Physics, University of California at San Diego, La Jolla, California 92093 and General Atomics, La Jolla, California 92138

(Received 8 October 1991; accepted 25 November 1991)

The properties of the spectral energy transfer for a two-dimensional fluid representation of dissipative trapped ion convective cell turbulence are studied numerically using a spectral method. It is established that the spectral energy flow is from long to short wavelength, as governed (under the dynamics of the $E \times B$ nonlinearity) by a single quadratic invariant, the energy. This flow is correctly predicted by equilibrium statistical mechanics, as is the equilibrium spectrum. Examining the locality of energy flow, strong nonlocal energy transfer is observed, a process that efficiently transfers the energy of a mode across the spectrum in a correlation time. This transfer process deviates dramatically from the canonical self-similar cascade dynamics of Kolmogorov that typifies the cascade of two- and three-dimensional Navier–Stokes and Hasegawa–Mima drift wave turbulence. Anisotropy of the spectral transfer dynamics is also observed.

I. INTRODUCTION

The possibility that turbulence driven by unstable trapped ion modes plays a role in core fluctuations and transport in tokamaks has generally been discounted throughout the past decade. At one time, however, trapped ion modes were thought to represent a potentially serious confinement problem for auxiliary heated (multikilovolt) plasmas.[1] Indeed, catastrophic Bohm-like transport was predicted. This prediction was premised on a presumed inverse cascade of energy from the already long wavelengths of the unstable fluctuations, and the fact that fluctuation levels would be large, given the long radial correlation length of the turbulence. The successful operation of the Princeton Large Torus device[2] at temperatures in excess of 4 keV without catastrophic confinement problems was generally taken as an indication that trapped ion mode activity was somehow absent from hot auxiliary heated tokamak discharges. Excepting some early efforts to explain this seeming lack of trapped ion mode turbulence[3] and some work on low collisionality ion-temperature-gradient-driven turbulence,[4] trapped ion turbulence has generally been ignored.

Recent work on trapped ion mode turbulence based on approximate analytic solution of renormalized Kadomtsev–Pogutse fluid equations[5] contends that these fluctuations cannot be discounted as an important component of core turbulence and may, in fact, comprise the low-frequency large-amplitude extreme of experimental spectra. Contrary to the predictions of Bohm-like transport,[1] this work asserts that trapped ion convective cell turbulence drives transport that is not excessively large, but is comparable in magnitude to the transport produced by trapped electron turbulence. This contention is supported by two facts. The first is that the turbulent radial flow associated with trapped ion convective cell turbulence is small, offsetting the large fluctuation level in the quadratic moments that determine the transport fluxes. The second is the prediction that spectral energy transfer is not characterized by an inverse cascade, but rather is directed to short wavelengths. The latter precludes catastrophic condensation of energy at the largest scales of the system.

There is mounting experimental evidence that fluctuations with large radial correlation length are present in the core of tokamak plasmas. Observed spectra from scattering diagnostics have long exhibited an increase of spectral energy toward the smallest resolved wave numbers, typically with no turnover evident over the range of wave numbers for which measurement is possible. Recently, new fluctuation diagnostics with the capability of providing spatially resolved local measurements of core turbulence have been developed. Both beam emission spectroscopy[6] and correlation reflectometry[7] find evidence for fluctuations inside r/a of 0.7 with radial correlation lengths of several centimeters. In both cases, the frequency of the fluctuations is very low or nearly zero, once the rotation induced Doppler shifts are subtracted. Intriguing links with global confinement are evident. While it has not been possible to associate these fluctuations with any given model, trapped ion convective cell turbulence is clearly a candidate.

In this paper, we describe a numerical study of dissipative trapped ion convective cell turbulence. Motivated by the issue of the energy transfer direction in wave number space for trapped ion turbulence, key facets of the spectral energy transfer process are examined. In order to isolate basic physical processes and enable comparison with analytic theory, a simple two-dimensional (2-D) single field model is utilized. This model is based on the fluid responses for trapped ions and electrons first used by Kadomtsev and Pogutse. The link between electrons and ions provided by quasineutrality enables a single field description. Rapid trapped particle bounce motion, restricting the development of parallel dynamics, provides the rationale for a two-dimensional treat-

 0899-8221/92/030599-12$04.00

ment. The model incorporates the $E \times B$ nonlinearity, the dominant nonlinear transfer mechanism for long wavelength fluid plasma turbulence. Consequently, the turbulent transfer properties of dissipative trapped ion convective cell turbulence, as described by the model, apply to a broader class of long wavelength fluctuations, including those resulting from trapped electron modes.

In addition to determining the direction of energy transfer in wave number space, an investigation of other properties relating to the spectral transfer process is described in detail. This includes the degree to which transfer in wave number space is local, as implicit in Kolmogorov-type similarity arguments, which envision an energy transfer through all scales at precisely the same rate; or nonlocal, and therefore at variance with the standard view of cascades. The degree of isotropy or anisotropy in the energy transfer process and in the spectrum itself is also investigated. Finally, the direction of energy transfer is examined in relation to the quadratic invariants of the nonlinearity and the equilibrium spectrum. The latter ties in with statistical mechanics calculations frequently used to infer the direction of cascades.[8,9] Clearly, these properties impact the spectrum, the turbulence level, and the magnitude of spatial transport. At a more fundamental level, they affect the basic characterization of turbulence and turbulent cascades.

Spectral transfer and its characterization in terms of cascades has long been a central part of the conceptualization of turbulence. In Navier–Stokes turbulence, for example, it is well established that the energy transfer can be represented by a self-similar cascade process. In three dimensions, this process conservatively transfers energy to small scales. In two dimensions, the invariance of an additional quantity, enstrophy, or mean square vorticity, precludes the self-similar transfer of energy to small scale. It is possible to conserve both quantities, however, if enstrophy is transferred to small scale and energy to large scale. By analogy with 2-D Navier–Stokes turbulence, it might be inferred (mistakenly, as will become apparent) that dissipative trapped ion convective cell turbulence undergoes an inverse energy cascade (cascade to long wavelength). However, it is the simultaneous invariance of energy and enstrophy that directly underlies the dual cascade of 2-D Navier–Stokes turbulence and not the number of dimensions (except through the number of invariants).

It is often possible to infer the direction of spectral transfer from closure equations. These describe the average transfer consistent with the statistical ansatz invoked to obtain the closure. The statistical hypotheses upon which closures are predicated are, in general, very difficult to validate and are known to be violated by fluctuations that are spatially intermittent. Furthermore, a number of other approximations and simplifications typically enter into analytical results obtained from closure equations. In particular, the closure is most often applied to one-point equations. While one-point analyses simplify the determination of a saturation level, they neglect the incoherent transfer process required for energy conservation. For these reasons, other methods for inferring the spectral transfer have been developed.

The most widely used method is based on equilibrium statistical mechanics.[8,9] This method is appealing for its direct use of the dynamical invariants in obtaining equilibrium spectra of the invariant quantities. Its weakness lies in the somewhat tenuous connection between equilibrium quantities and the properties of turbulence, which generally are far from equilibrium. At the minimum, the use of an equilibrium spectrum to infer a spectral transfer direction requires a knowledge of the steady state spectrum set up under forcing and dissipation, and the assumption that nonlinear transfer in the steady state is in the direction that would tend to drive the spectrum toward its equilibrium configuration. An additional weakness arises from the possibility that additional invariants exist that constrain the transfer but are not among those known and included in the calculation of the equilibrium spectrum, thereby compromising the equilibrium prediction. Not withstanding these difficulties, equilibrium statistical mechanics correctly predicts the direction of spectral transfer in two-dimensional and three-dimensional (3-D) Navier–Stokes turbulence,[8,9] and has been used in many other types of turbulence.[10,11]

In the present work, nonlinear transfer in the numerical simulation of the Kadomtsev–Pogutse fluid model is directly measured in distinct regions of wave number space. In order to eliminate the transfer imposed by any particular wave number space distribution of sources and sinks in favor of the conservative transfer produced by the nonlinearity, transfer is determined for undriven/undamped turbulence starting from a finite-amplitude initial state with a given spectrum. These results establish the direction of inertial transfer of energy in a steady state whose spectrum is similar to the spectrum chosen as an initial condition. The initial spectrum relaxes under the inertial transfer, producing time asymptotically an equilibrium spectrum that can be compared with the spectrum predicted by equilibrium statistical mechanics on the basis of the known dynamical invariants. These studies therefore provide a test of the validity of the methodology of equilibrium statistical mechanics for predicting spectral transfer directions, as well as a check on the predictions of the closure theory.

The concept of a wave number cascade is usually thought of as a local process, whereby energy is passed between scales that are adjacent in wave number space. The renormalized Kadomtsev–Pogutse equation provides for both local and nonlocal transfer of internal energy $|\tilde{n}_k|^2$ in wave number space. According to the renormalized equation,

$$\frac{1}{2}\frac{\partial |\tilde{n}_k|^2}{\partial t} - \gamma_k |\tilde{n}_k|^2 + T_k = 0, \tag{1}$$

the evolution of energy in the mode k is governed, apart from linear driving and damping (γ_k), by a transfer rate T_k with local and nonlocal components. Specifically, the transfer rate, as given from a standard statistical closure, is

$$T_k = \sum_{k'} |\tilde{n}_k|^2 |\tilde{n}_{k'}|^2 [A_{\mathrm{NL}}(k,k') + A(k,k')] + \sum_{p+q=k} |\tilde{n}_p|^2 |\tilde{n}_q|^2 A(p,q), \tag{2}$$

where

$$A_{\mathrm{NL}}(k,k') = \mathrm{const}(\mathbf{k}\times\mathbf{k}'\cdot\mathbf{z})^2 \mathscr{L}_{k,k'}^{-1}(k_y'^2 - k_y^2),$$
$$A(k,k') = \mathrm{const}(\mathbf{k}\times\mathbf{k}'\cdot\mathbf{z})^2 \mathscr{L}_{k,k'}^{-1} k_y'^2,$$

are coupling coefficients, and reflection symmetry in k_y has been assumed for convenience in this discussion. Aside from the $E\times B$ geometrical factor $(\mathbf{k}\times\mathbf{k}'\cdot\mathbf{z})^2$ and the nonlinear response time $\mathscr{L}_{k,k'}^{-1}$ (to be defined in the next section), these coefficients are governed by the factors $(k_y'^2 - k_y^2)$ and $k_y'^2$. The factor in A_{NL} indicates transfer that is negligible for k comparable to k', but large for disparate values, i.e., transfer that is nonlocal. Also, the sign of A_{NL} is such that energy is depleted from the mode k when $k_y'^2 > k_y^2$, and deposited into that mode when $k_y'^2 < k_y^2$. This clearly implies transfer to large wave number. By contrast, the factor in A is positive definite, indicating transfer that is always out of (rather than into) the mode k, and independent of the relative positions of k and k' in wave number space. (Note that for this term, nonlocal transfer is *not* precluded.)

The strong interaction and direct energy exchange between modes of widely disparate wave numbers suggested by A_{NL} is a fundamental departure from the cascade dynamics implicit in steady state spectra formulated according to the similarity concepts of Kolmogorov. If nonlocal transfer dominates, it is possible that the steady state wave number spectrum in an inertial range will strongly deviate from a self-similar spectrum. It is difficult to determine precisely the relative magnitudes of local and nonlocal transfer from renormalized equations without knowing the spectrum. Moreover, nonlocal transfer may be offset by the term A, which is not restricted to purely local triads. In the simulations, nonlocal and local transfer rates are directly measured throughout the relaxation.

The dominant nonlinearity governing mode coupling at long wavelengths is the $E\times B$ nonlinearity. This nonlinearity is anisotropic with respect to the two cross-field directions. The anisotropy carries over to the closure equations, where highly anisotropic transfer, particularly nonlocal, is evident. In contrast, the equilibrium spectrum, derived from a single isotropic invariant (energy) is isotropic in the two cross-field directions. This seeming contradiction is examined in detail from the simulation results in order to determine the degree of anisotropy in the spectrum and local and nonlocal transfer rates.

The results of this paper are now summarized. Inertial energy transfer by trapped ion convective cell turbulence has been examined numerically for a 2-D Kadomtsev–Pogutse fluid model. Numerical solution of the equations was accomplished with a spectral code containing up to 41×41 modes. The spectrum evolution and transfer rate time histories of spectra initially peaked at low wave number were observed with two distinct regimes of evolution in evidence. In the first, there is a strong transfer of energy to high wave number occurring over several eddy turnover times and resulting in the relaxation of the spectrum to a configuration with noticeable peaking at high k_y (y is the cross-field direction perpendicular to the inhomogeneity in density). Nonlocal transfer in k_y plays an important role in the relaxation process and is responsible for the peaking in k_y. Enstrophy increases throughout this regime. In the second regime the spectrum further relaxes to an approximately equipartitioned state under the action of sloshing in wave number space. The final spectrum is roughly consistent with the predictions of equilibrium statistical mechanics based on a single invariant corresponding to the internal energy. A slight peaking in k_y is apparent in this time-asymptotic spectrum. The peaking represents a minor deviation from the predicted equilibrium spectrum, but one that strengthens, rather than weakens, the equilibrium statistical mechanics prediction that energy transfer is to small scale. For an initial spectrum that is flat, net transfer to small scale in the k_y direction is again evident, but is weaker than that of the peaked spectrum case. This transfer is highly nonlocal, producing a spectrum that is slightly peaked in k_y and similar to the spectrum of the sloshing regime when reached from a peaked initial condition. The flat initial spectrum case is important because stationary turbulence driven at long wavelengths, damped at short wavelengths, and having an inertial range in intermediate scales, results in a stationary spectrum that is only weakly peaked at low k.

Nonlocal transfer in k_y derives from the direct coupling of modes, which are widely separated in wave number space. For initial spectra with indices α less that 3, where $|n|^2 = k_y^{-\alpha}$, the nonlocal transfer in k_y dominates local transfer, thus invalidating Kolmogorov similarity range arguments for inertial range transfer. For $\alpha > 3$, the coupling between disparate scales is strongly reduced by the large-amplitude disparity and transfer is dominantly local until the spectrum has relaxed to $\alpha \sim 3$. The local and nonlocal rates are comparable in the k_x direction. This represents a pronounced anisotropy in the spectral transfer of energy. Because the local transfer tends to be isotropic, anisotropies in the spectrum are less pronounced.

The remainder of this paper is organized as follows: the basic model, its properties, and the basic computational procedure are presented in Sec. II. In Sec. III, the equilibrium spectrum and similarity-range stationary spectrum are derived and the prediction for spectral transfer direction is formulated. The simulation results are detailed in Sec. IV, and conclusions are given in Sec. V.

II. BASIC EQUATIONS AND COMPUTATIONAL PROCEDURE

In order to study nonlinear processes in detail, a simple model is used. This model, based on Kadomtsev–Pogutse equations, treats dissipative trapped ion convective cell turbulence as a turbulent fluid described by a single scalar related to both the fluctuating density and the flow streamfunction (electrostatic potential). This model therefore allows contact with the considerable body of knowledge existing for Navier–Stokes turbulence and similar fluid plasma models, such as the Hasegawa–Mima equation[12] and its dissipative analogs.[13] At the same time, the model is sufficiently complete to capture many essential elements of trapped ion turbulence. The model equation is given by

$$\frac{\partial \tilde{n}}{\partial t} + D\frac{\partial^2 \tilde{n}}{\partial y^2} + \frac{V_D}{2}\frac{\partial \tilde{n}}{\partial y} + \nu_{\text{eff},e}\tilde{n} - \frac{4L_n D}{\epsilon^{1/2}}\nabla\frac{\partial \tilde{n}}{\partial y}\times\mathbf{z}\cdot\nabla\tilde{n} = 0, \tag{3}$$

where $\tilde{n} = \epsilon^{1/2} n^{\text{tr}}/n_0$ is the normalized trapped ion density, $V_D = \epsilon^{1/2}(cT_i/eB)L_n^{-1}$ is the effective diamagnetic drift velocity for trapped ions, $D = V_D^2/4\nu_{\text{eff},e}$ is an inverse diffusivity describing the destabilization of trapped ion modes by electron collisions, $\nu_{\text{eff},i}$ is the effective collision frequency of ion–ion collisions with $\nu_{\text{eff},j} = \nu_j/\epsilon$, $\epsilon = r/R$ is the inverse aspect ratio parametrizing the fraction of trapped particles, and L_n is the density gradient scale length. This equation incorporates the dynamics of both trapped electrons and trapped ions with quasineutrality providing the link between their densities. The turbulent fluid flow is the $E\times B$ flow. This flow couples to the density fluctuations through the $E\times B$ advection of the mean density gradient.

The electron dynamics incorporates adiabatic (passing) and nonadiabatic (trapped) electrons. As a result of the very low frequency of the fluctuations, the trapped electrons are collisional, i.e., trapped electrons experience multiple collisions over a fluctuation period. Consequently, electron dynamics are governed by collisional scattering as opposed to nonlinear advection. This results in a linear relation between the fluctuation source (given by the $E\times B$ advection of the average density) and the trapped electron density. Trapped electrons are therefore laminar, with a density that is proportional to the potential and 90° out of phase due to the collisions. Electron collisions access the density gradient free energy through an inverse damping process and thus provide the basic instability that feeds the turbulence.

The combination of electron and ion densities into a single field using the laminar electron response constitutes an "$i\delta$" approximation ($\tilde{n}_e \sim i\delta\phi$, where $\delta = 4L_n D/\epsilon^{1/2}$ is the nonadiabatic electron response). It is worth noting that because electron inertia is negligible, the nonadiabatic electron response, or function δ, has no explicit dependence on the frequency. Thus, the need to approximate the nonadiabatic response by evaluating an explicit frequency dependence at ω_* or a linear frequency does not arise. Explicit frequency dependence in other types of drift-wave fluctuations (collisionless trapped electron modes, universal modes, etc.) represents a serious shortcoming of the $i\delta$ approximation, but one that does not occur in the present case.

The ion response is hydrodynamic and consists of $E\times B$ advection, the polarization drift, and ion–ion collisions. The latter affects the fluctuations at very long wavelengths, providing a low k cutoff for the instability. The long wavelengths of the fluctuations restrict the extent to which the polarization drift plays any role in the dynamics. As a consequence, the fluctuations are essentially nondispersive in the energy containing scales fed by the instability. Similarly, the polarization drift nonlinearity $[n_0\nabla\cdot\mathbf{v}_p^{(1)}$, where $\mathbf{v}_p^{(1)} = B_0^{-1}(c/e)\mathbf{z}\times\mathbf{v}_E\cdot\nabla\mathbf{v}_E$ and $\mathbf{v}_E = -\nabla\phi\times\mathbf{z}]$, familiar from the Hasegawa–Mima equation, is small compared to the $E\times B$ nonlinearity ($\mathbf{v}_E\cdot\nabla\tilde{n}_i$). The $E\times B$ nonlinearity is nonzero only through the nonadiabatic electron response and produces dissipative coupling, which breaks enstrophy conservation.[13] The $E\times B$ nonlinearity dominates at long wavelengths where $k\rho < \delta$ (ρ is the ion gyroradius at the electron temperature). The present study is concerned with the long wavelength limit, so only the $E\times B$ nonlinearity is retained in the model. Because energy transfer in regions dominated by the $E\times B$ nonlinearity is toward small scales (a principal conclusion of this paper), energy eventually reaches regions where the polarization drift nonlinearity becomes important and other effects occur, such as coupling to smaller wavelength trapped electron modes. Future work will address the dynamics at shorter wavelengths where the two nonlinearities participate in the transfer process.

As indicated previously, the Kadomtsev–Pogutse equation, Eq. (3), accurately represents many essential elements of trapped ion turbulence. These include the correct electron dissipation-induced linear growth rate of the driving instability. The linear frequency is also correctly represented as nondispersive, in the direction of the electron diamagnetic drift, and offset from the diamagnetic frequency by the trapped particle fraction. Energy transfer is appropriately governed by the $E\times B$ nonlinearity. This model does not account for parallel dynamics (and hence radial mode structure) or coupling to short wavelength fluctuations.

The computational method employed is spectral. Thus the time evolution of Fourier modes (coupled by the convolution sum of the $E\times B$ nonlinearity) is solved according to

$$\frac{\partial \tilde{n}_k}{\partial t} = Dk_y^2\tilde{n}_k - i\frac{V_D}{2}k_y\tilde{n}_k - \nu_{\text{eff},e}\tilde{n}_k - \frac{4iL_nD}{\epsilon^{1/2}}\sum_{\mathbf{k}'}(\mathbf{k}\times\mathbf{k}'\cdot\mathbf{z})k_y'\tilde{n}_{k'}\tilde{n}_{k-k'}. \tag{4}$$

A truncation of Fourier space limits the spatial resolution of the solution. Time advancing is accomplished using a gear-type solver with an explicit Jacobian. The code is purely spectral, treating Eq. (4) as it is written, as opposed to pseudospectral, which uses fast Fourier transforms to calculate the convolution term in real space, where the fields are a simple product. The use of a spectral method limits the resolution relative to that possible with a pseudospectral code; however, subtle issues involving dealiasing are thus avoided. In particular, pseudospectral methods require dealiasing, a process that distorts the Fourier modes in the shorter wavelength part of the spectrum. The portion of the spectrum that is usable is affected by anisotropies in the nonlinear coupling, and has subtleties which depend on whether the spectrum represents second-order moments such as energy, or higher-order moments.[14] In the present work, the energy and enstrophy *transfer* rates are computed. These quantities are calculated from triplet correlations. The effect of dealiasing on third-order correlations with anisotropic coupling is not well documented and for the purpose of developing such diagnostics, the spectral environment provides easier implementation and more reliable interpretation. The results presented here are obtained using a maximum of 41×41 modes. For the study of spectrum relaxation and energy transfer in turbulence that is undriven/undamped, this resolution is adequate, as verified by changing the number of modes.

A key feature of the computations reported in this paper is the calculation of the energy and enstrophy transfer rates

T_k and U_k in wave number space. Energy and enstrophy are defined as $\Sigma_k|\tilde{n}_k|^2$ and $\Sigma_k k^2|\tilde{n}_k|^2$. Thus, rates of energy and enstrophy transfer from a given mode k are obtained by multiplying the last term of Eq. (4) by $\tilde{n}_k^*$ and $k^2\tilde{n}_k^*$ giving, respectively,

$$T_k = \frac{4iL_nD}{\epsilon^{1/2}} \operatorname{Im} \sum_{\mathbf{k}'} (\mathbf{k}\times\mathbf{k}'\cdot\mathbf{z}) k_y' \tilde{n}_{k'}\tilde{n}_{k-k'}\tilde{n}_k^* \qquad (5)$$

and

$$U_k = \frac{4iL_nD}{\epsilon^{1/2}} \operatorname{Im} \sum_{\mathbf{k}'} (\mathbf{k}\times\mathbf{k}'\cdot\mathbf{z}) k^2 k_y' \tilde{n}_{k'}\tilde{n}_{k-k'}\tilde{n}_k^*. \qquad (6)$$

These quantities are evaluated at each step of the computation yielding instantaneous rates of transfer between the mode k and all other coupled modes in the spectrum. Positive T_k represents a net flow of energy into the mode k; negative T_k represents net outflow. Because energy is conserved by the nonlinear transfer, the energy flow into or out of a mode must be equal to the flow out of or into all remaining modes. Enstrophy, on the other hand, is not conserved. If energy is transferred conservatively to short wavelength, as occurs in 3-D Navier–Stokes turbulence, it follows from simple dimensional arguments that enstrophy will be generated. If energy flows to long wavelength, the converse will hold. Consequently, the evolution of total enstrophy, obtained from the time history of $\Sigma_k U_k$, provides an additional indicator of energy transfer direction and is the principal enstrophy diagnostic utilized.

The closure representation of the energy transfer rate [Eq. (2)] follows from Eq. (5) by a straightforward iteration on each of the density fluctuation factors. Consistent with quasi-Gaussian statistics, the iterated density factors, or driven fluctuations, are directly excited by a single triplet interaction, with the remaining triplets acting to nonlinearly decorrelate the interaction. The directly acting triplet is the one yielding closure, e.g.,

$$\mathcal{L}_{k-k'}\tilde{n}_{k-k'} = -(4iL_nD/\epsilon^{1/2}) \times (\mathbf{k}'\times\mathbf{k}\cdot\mathbf{z})(k_y + k_y')\tilde{n}_k\tilde{n}_{k'},$$

where $\mathcal{L}_{k-k'}$ is the nonlinearly broadened propagator, consisting of linear growth, damping, diamagnetic rotation, and the nonlinear decorrelation. Carrying out this procedure yields

$$T_k = \left(\frac{4L_nD}{\epsilon^{1/2}}\right)^2 \sum_{\mathbf{k}'} (\mathbf{k}'\times\mathbf{k}\cdot\mathbf{z})^2 k_y'(k_y' - k_y)\mathcal{L}^{-1}_{k,k',k-k'}|\tilde{n}_k|^2|\tilde{n}_{k'}|^2 + \left(\frac{4L_nD}{\epsilon^{1/2}}\right)^2 \times \sum_{\mathbf{k}'} (\mathbf{k}'\times\mathbf{k}\cdot\mathbf{z})^2(k_y'^2 - k_y^2)\mathcal{L}^{-1}_{k,k',k-k'}|\tilde{n}_k|^2|\tilde{n}_{k'}|^2 + \left(\frac{4L_nD}{\epsilon^{1/2}}\right)^2 \sum_{\mathbf{p}+\mathbf{q}=\mathbf{k}} (\mathbf{p}\times\mathbf{q}\cdot\mathbf{z})^2 p_y(p_y - q_y)\mathcal{L}^{-1}_{k,p,q}|\tilde{n}_p|^2|\tilde{n}_q|^2, \qquad (7)$$

where

$$\mathcal{L}^{-1}_{k,k',k-k'} = i(\omega_{k'} + \omega_{k-k'} + \omega_{-k} - \gamma_{k'} - \gamma_{k-k'} - \gamma_{-k} + \Delta\omega_{k'} + \Delta\omega_{k-k'} + \Delta\omega_{-k})$$

is the triplet interaction correlation time, $\gamma_k = Dk_y^2 - \nu_{\mathrm{eff},e}$ is the linear growth rate, and

$$\Delta\omega_k = [(4L_nD)^2/\epsilon] \sum_{k'} (\mathbf{k}'\times\mathbf{k}\cdot\mathbf{z})^2 k_y'^2 \times \mathcal{L}^{-1}_{k,k',k-k'}|\tilde{n}_{k'}|^2$$

is the nonlinear decorrelation rate.

The first term of Eq. (7) comes from the iteration of $\tilde{n}_{k-k'}$ and describes advection of density by the turbulent flow. The third term arises from the iteration of $\tilde{n}_k^*$ and incorporates the incoherent transfer process neglected in one-point closures.[15] The second term is obtained by iterating on $\tilde{n}_{k'}$, the fluctuation representing the turbulent flow $[\tilde{v}_{k'} \propto ik_y\tilde{n}_{k'}]$. Consequently, this term provides for the self-consistent back reaction of the density fluctuations on the turbulent flow. In closures of Vlasov–Poisson systems, this term represents the renormalization of the shielding cloud and is frequently neglected because it requires the solution of a nonlinear Poisson equation. In fluid treatments it has a similar meaning through the correspondence between flow and potential that underlies $E\times B$ motion. Likewise, it is often neglected in order to avoid a nonlinear eigenvalue problem. The nonlocal transfer produced by this term can be thought of as the interaction between large-scale flow (shielding potential) and smaller-scale density fluctuations. As noted in the Introduction, the nonlocal transfer is unequivocally toward small scale.

In order to reduce the data required to establish the direction of energy transfer and examine other properties of the transfer process, the transfer into or from bands in wave number space is measured by summing Eqs. (5) and (6) over selected k values. The bands are chosen to represent slices in k_x and k_y in order to be sensitive to any anisotropies in the wave number space transfer. With the band structure, it is possible to track local energy flow in k space through adjacent bands. Nonlocal transfer is also easily observed. The definition of local versus nonlocal transfer is somewhat difficult to quantify. Typically, nonlocal transfer is used to signify exchange of energy with modes in the discrete spectrum that are displaced by more than two or three wave numbers, i.e., an interaction with modes that are not nearest neighbors. However, with such a definition, observed nonlocal transfer could still be compatible with a self-similar transfer, provided it admitted a similarity range with a number of these nonlocal steps. In order to identify energy flow that is incompatible with a similarity range, nonlocal transfer will be defined as energy exchange in interactions spanning more than half (or occasionally one-third) of the inertial range. Local transfer will be the difference of the total transfer and the nonlocal transfer, i.e., the flow to modes that are not removed by approximately half of the k-space extent.

III. EQUILIBRIUM AND SIMILARITY RANGE SPECTRA

In this section, the prediction that trapped ion turbulence produces a transfer of energy to short wavelength[5] is reviewed. This prediction is based on a comparison of the equilibrium spectrum calculated from statistical mechanics, and the stationary spectrum describing the distribution of energy in a driven saturated state. The equilibrium spectrum is derived using the statistical probability distribution function for a canonical ensemble consistent with the known invariants of the nonlinearity. In applying these statistical tools, it is assumed that turbulent transfer in the steady state is in the direction in wave number space that would tend to drive the spectrum to the equilibrium configuration if the driving and damping were turned off. The testing of this assumption is one of the objectives of the present study. Clearly, the application of this method requires knowledge of the stationary spectrum established by the turbulently moderated balance of driving and damping. In this paper, the simplest stationary spectrum, consistent with a Kolmogorov-type similarity range, will be adopted as a benchmark. Because the validity of a similarity range spectrum is cast into doubt by the results of the next section, the issue of the appropriate stationary spectrum and its role in the prediction of transfer direction will be revisited at that time.

In the absence of driving and damping, a single nontrivial quadratic invariant is admitted by the Kadomtsev–Pogutse equation. This invariant is the internal energy, $\int d^2x\, n^2$, whose conservation follows from the fact that

$$\int \nabla \frac{\partial \tilde{n}}{\partial y} \times \mathbf{z} \cdot \nabla \tilde{n}\, d^2x = 0. \tag{8}$$

A second integral, $\int d^2x\, \partial \tilde{n}^2/\partial y$, is also conserved by the nonlinearity. However, by symmetry, this integral is identically zero for all time, and therefore imposes no constraint on the cascade dynamics. Enstrophy, an invariant of the 2-D Navier–Stokes and Hasegawa–Mima equations, is not conserved by the $E \times B$ nonlinearity. The nonconservation of enstrophy arises from the nonadiabatic electrons.[13]

With energy as the only nonzero quadratic invariant, the canonical probability distribution of equilibrium states is

$$P = \exp\left(-\frac{\beta}{2} \sum_{\mathbf{k}} |\tilde{n}_k|^2 \right), \tag{9}$$

where β is an effective inverse temperature. The spectrum is given by the expectation value of the energy in a mode k_j, yielding

$$|\tilde{n}_{k_j}|^2 = \frac{\int |\tilde{n}_{k_j}|^2 P\, d\tilde{n}_{k_1}\, d\tilde{n}_{k_2} \cdots d\tilde{n}_{k_{\max}}}{\int P\, d\tilde{n}_{k_1}\, d\tilde{n}_{k_2} \cdots d\tilde{n}_{k_{\max}}}. \tag{10}$$

Equation (10) predicts an equipartition of the energy,

$$|\tilde{n}_k|^2 = 1/\beta, \tag{11}$$

corresponding to a flat spectrum in the 2-D wave number space. In addition to equipartition, the equilibrium spectrum is isotropic, a feature that follows from the fact that the lone nonzero quadratic invariant has no explicit anisotropy.

As stated previously, a similarity range stationary spectrum is calculated for comparison with the equilibrium spectrum. Assuming that unstable modes are confined to a localized region of wave number space where $\omega < \omega_{bi}$, the balance of nonlinear transfer of energy $\tilde{n}^2$ at each scale in the spectrum with the net energy input rate requires that $\epsilon = k^3 \tilde{n}_k^3$, where ϵ is the fixed energy input rate and isotropy has been assumed, i.e., $\partial/\partial x = \partial/\partial y \to k$. Solving for $\tilde{n}_k^2$ and expressing in terms of an isotropic integral distribution for a single wave number k [$\int E(k)dk = \tilde{n}^2$], the spectrum is

$$E(k) = \epsilon^{2/3} k^{-3}. \tag{12}$$

If the spectrum is anisotropic ($\partial/\partial x \neq \partial/\partial y$), the balance of energy input rate with spectral transfer requires that $\epsilon = k_y^2 k_x \tilde{n}_k^3$. Writing the spectrum as an integral distribution in two wave numbers [$\int E(k_x,k_y)dk_x\, dk_y = \tilde{n}^2$] yields

$$E(k_x,k_y) = \epsilon^{2/3} k_x^{-5/3} k_y^{-7/3}. \tag{13}$$

Note that the second spectrum is consistent with the first and reduces to it when $k_x = k_y$. It has an additional power of k^{-1} because it is a distribution of energy in a two-dimensional wave number space. In contrast to the equilibrium spectrum, both similarity range spectra are peaked at long wavelength. The anisotropy in k_x and k_y of Eq. (13) arises directly from the anisotropy of the $E \times B$ nonlinearity. These spectra follow for an inertial cascade, regardless of its direction in wave number space. Assuming that the nonlinear interactions of the inertial range attempt to drive the system toward equilibrium, transfer will be in such a direction as to establish the equilibrium spectrum, $E \sim \beta^{-1}$. On this basis, transfer is predicted to be toward short wavelength. If a similarity range does not exist, but the stationary spectrum of driven turbulence remains peaked at the long wavelength, the transfer is again predicted to be toward short wavelength.

The transfer of energy to short wavelength is a consequence of the existence of a single quadratic invariant. By contrast, the 2-D Navier–Stokes and Hasegawa–Mima equations have two invariants and thus a canonical probability distribution function that depends on the two integrals. The equilibrium spectra calculated from this distribution function have enstrophy weighted toward short wavelengths and energy weighted toward long wavelengths. Consequently, enstrophy in these systems is predicted to flow to short wavelengths and energy to long wavelengths.

IV. COMPUTATIONAL RESULTS

The results reported in this section come principally from numerical experiments in which turbulence is initialized with finite amplitude in a variety of spectral distributions and allowed to evolve with no forcing or dissipation. Initial spectra range from k^{-1} to k^{-6}, bracketing the similarity range stationary values of $k_x^{-5/3} k_y^{-7/3}$. Evolution is tracked for as many as 100 eddy turnover times. In all cases, the initial spectra relax to an identical time-asymptotic configuration. The instantaneous flow during the spectrum evolution is measured to indicate the flow that would occur in a driven/damped stationary situation having a spectrum like the instantaneous spectrum during relaxation. The time history of energy is calculated throughout the runs as a check on the numerics. Energy is found to be conserved to better

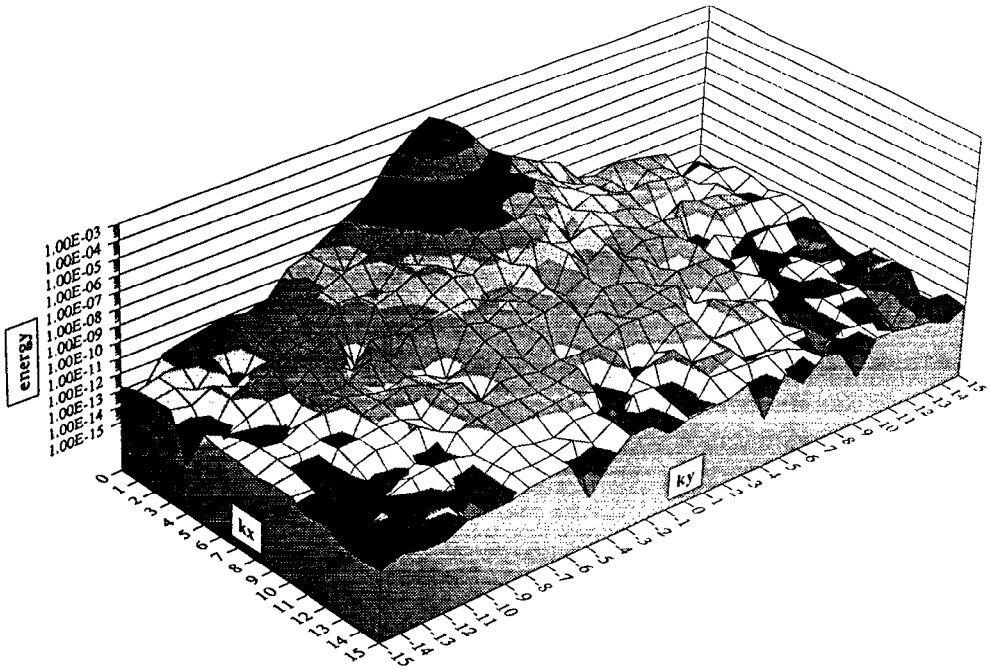

FIG. 1. Spectrum of undriven/undamped turbulence at the initial time. The initial phases are random and the initial spectrum fall-off index is $\alpha = -4$.

than one part in 10^8 for tens of eddy turnover times. The nonlinear transfer diagnostics have also been benchmarked against hand calculations for a small k space in order to verify their accuracy.

The time-asymptotic spectrum is found to be flat, in very good agreement with the predicted equilibrium spectrum. This agreement is remarkable, given that the nonlinearity that drives the relaxation and the measured wave number space flow are anisotropic; yet the final spectrum is isotropic and in good agreement with a prediction that takes no account of the anisotropy in the nonlinearity. Figures 1–3 show a sequence of spectra, starting with an initial spectrum given by $E(k) = k^{-4}$, an intermediate configuration that occurs a few mean fluctuation time scales after the initial time, and an equipartitioned time-asymptotic spectrum corresponding to a fully relaxed state achieved tens of eddy turnover times after the initial time.

The spectra in Figs. 2 and 3 represent two distinct regimes of nonlinear transfer. The first is a flow regime characterized by robust transfer to high k_x and k_y. The k_y transfer is strongly nonlocal and is responsible for the peak and valley at high and intermediate k_y values, respectively, which is

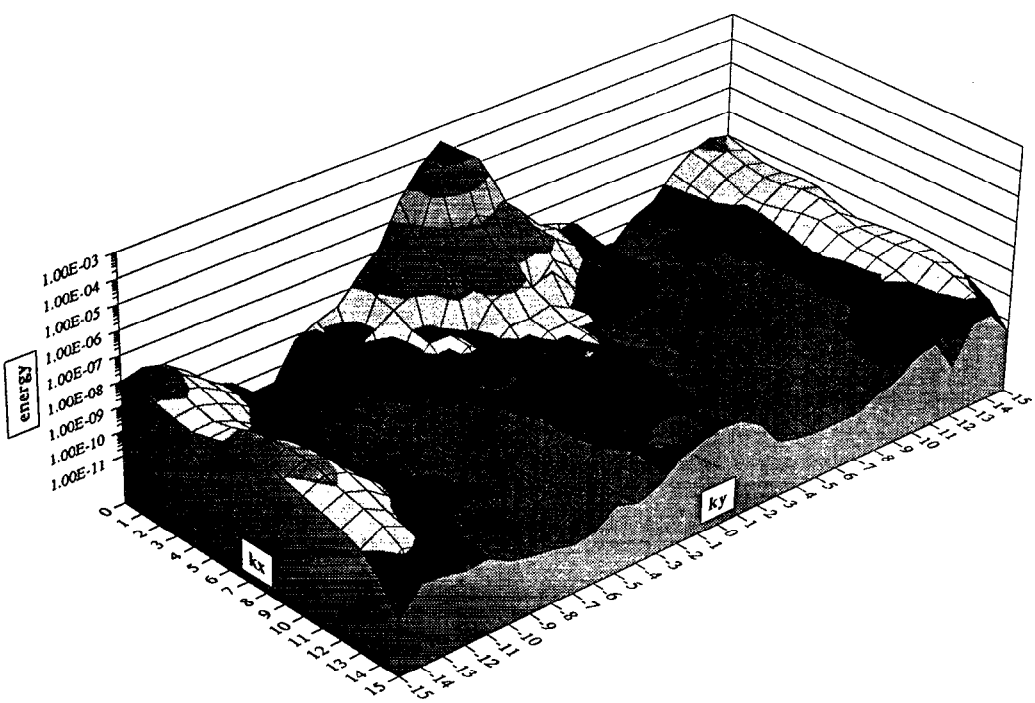

FIG. 2. Spectrum of undriven/undamped turbulence toward the end of the flow regime and just prior to the beginning of the sloshing regime. Approximately five to ten correlation times have elapsed from the initial time.

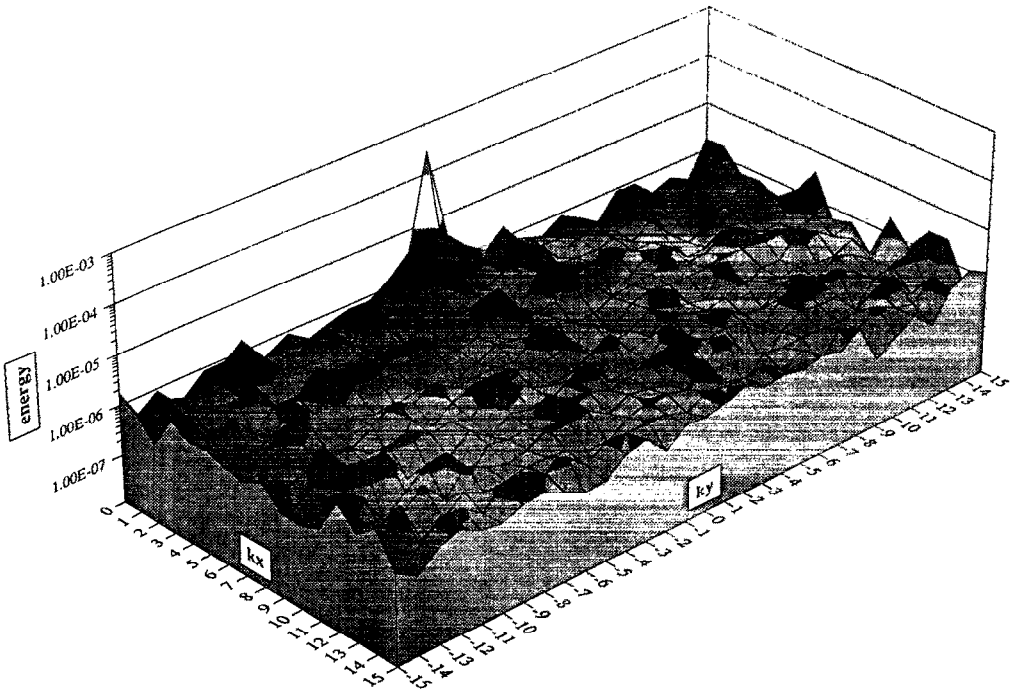

FIG. 3. Spectrum of undriven/undamped turbulence in the sloshing regime. The spectrum has been averaged over several correlation times. This spectrum is in the time-asymptotic (relaxed) configuration. (The central peak is the mode $k_x = k_y = 0$. Because this mode does not couple to any other mode, it retains its initial energy.)

evident in Fig. 2. The flow regime terminates five to ten eddy turnover times after the beginning of nonlinear transfer when all energy in the low k modes above the equilibrium value has been transferred to high k, thus depleting the low k spectrum peak. There is a noticeable peak at high k_y in the spectrum at the end of the flow regime. This is due to the relatively greater efficiency of the nonlocal k_y transfer, compared to the local transfer of the k_x flow. Because the spectrum at the end of the flow regime is anisotropic and not quite at the equilibrium configuration, a second regime ensues, characterized by sloshing of energy in wave number space. The sloshing regime exhibits rapid transfer of energy between modes, but with little net transfer. The spectrum is quickly isotropized and flattened by the sloshing. The time-asymptotic spectrum is nearly flat with a slight peak at high k_y. The sloshing interaction incorporates a wide range of time scales, from an eddy turnover time to hundreds of eddy turnover times. The sloshing motion roughly produces the equipartitioned spectrum predicted by equilibrium statistical mechanics. However, this regime is probably not relevant to the transfer occurring in a driven stationary state. Insofar as the nonlinear transfer of the steady state is concerned, it is essentially an artifact of the finite (truncated) k space coupled with the efficient nonlocal transfer, and the fact that there is no dissipation at short wavelengths to absorb the energy nonlinearly transferred from long wavelengths.

While the two regimes of nonlinear transfer have a noticeable effect on the spectrum, their properties are most clearly seen in the energy transfer and enstrophy production diagnostics. Figure 4 shows the net energy transfer from bands of constant k_y and k_x in both the long and short wavelength parts of the spectrum. The flow regime is clearly apparent as the period over which there is a continuous outflow from low k, as evidenced by the negative value of T_k for the long wavelength bands, and an inflow to high k, as seen in the positive value of T_k for the short wavelength bands. After $t = 2.5$, the sloshing regime is reached and the transfer is oscillatory with no net sign apparent. Figure 5 indicates that the enstrophy production rate is positive throughout the flow regime and saturates at the transition to the sloshing regime. Positive enstrophy production results from the conservative transfer of energy from long to short wavelength, with the net increase of enstrophy proportional to the ratio

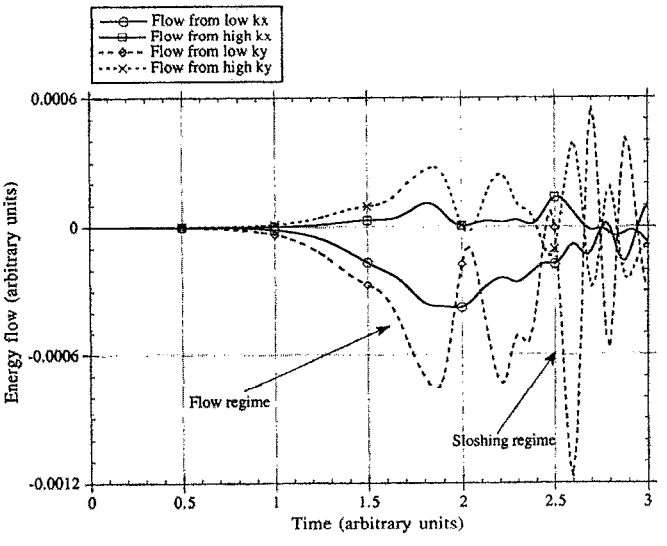

FIG. 4. Net energy transfer rates for long and short wavelength bands of constant k_y and k_x. Energy is seen to flow out of the long wavelength bands (T_k negative) and into the short wavelength bands (T_k positive). Distinct flow and sloshing regimes are identifiable.

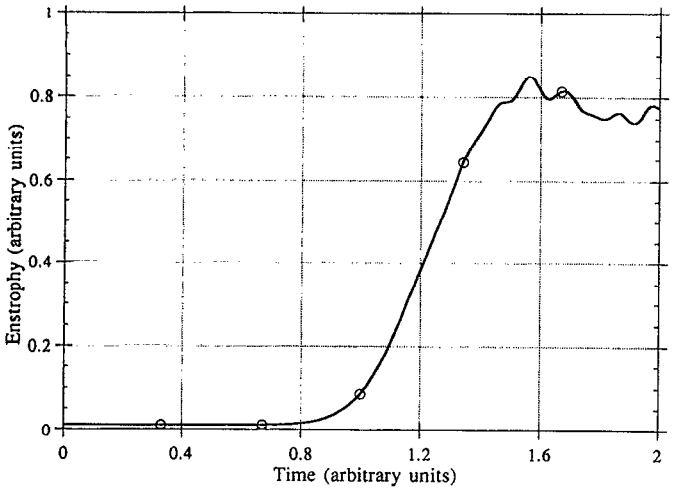

FIG. 5. Time evolution of the enstrophy. Enstrophy production is clearly evident in the flow regime, coinciding with energy transfer to long wavelength.

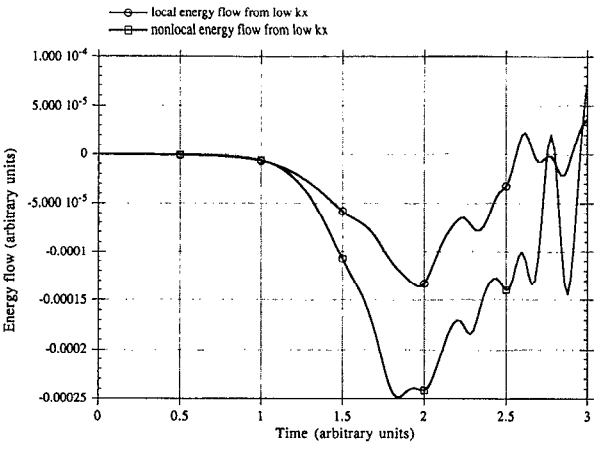

FIG. 7. Local and nonlocal transfer rates in the k_x direction. The parity of local and nonlocal transfer rates in the k_x direction and the disparity of local and nonlocal transfer rates in the k_y direction indicates a clear anisotropy in the transfer process.

$k^2_{\max}/k^2_{\min}$. The observed positive enstrophy production rate thus corroborates the results of the energy flow diagnostic. Note that the negative enstrophy production rate occurring transiently at the onset of sloshing coincides with the first wave of back-transfer.

Nonlocal transfer and its magnitude relative to local transfer is now examined. Figure 6 shows the time evolution of local and nonlocal transfer rates from a long wavelength $k_y = \text{const}$ band. By symmetry, transfer measured from a k_y band is dominantly the transfer in the k_y direction. From Fig. 6, the transfer in the flow regime is almost entirely nonlocal with a small local component. The initial spectrum in this case is $|\tilde{n}_k|^2 \sim k^{-4}$. Given the definition of nonlocal used in this study, this figure indicates that energy is efficiently passing directly from the low k_y modes to modes that are more than one-half of the wave number space removed. Stated in terms of the wave number triangles for the nonlinear interaction of k, k', and $k - k'$, triangles that are highly elongated are strongly favored over equilateral triangles in carrying the energy to high k_y. By contrast, Fig. 7 indicates that the transfer from a long wavelength band with $k_x = \text{const}$ is divided roughly equally between local and nonlocal components. There is therefore a pronounced anisotropy in the energy transfer process during the flow regime.

The anisotropy in transfer is also evident in the evolution of isodensity contours throughout the relaxation. Figures 8–10 show isodensity contours at the initial time, in the flow regime, and in the sloshing regime when the spectrum has reached equilibrium in an average sense. As expected, the initial isodensity contour plot has just one or two struc-

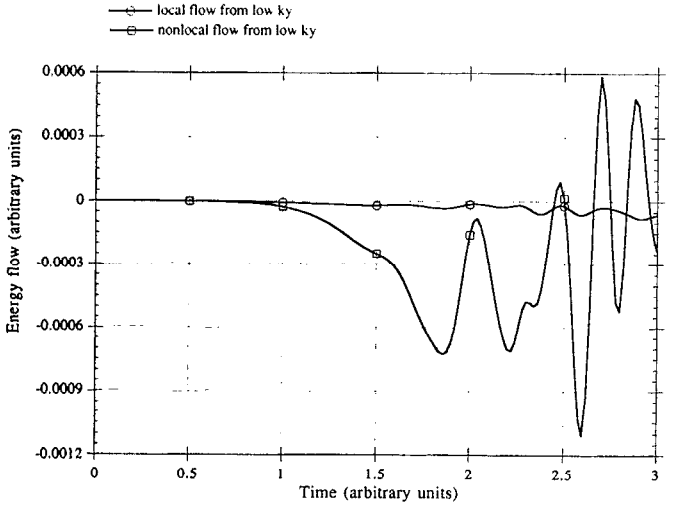

FIG. 6. Local and nonlocal transfer rates in the k_y direction. Transfer is clearly dominated by the nonlocal process, which here is defined as transfer between coupled modes separated by more than half of the wave number space.

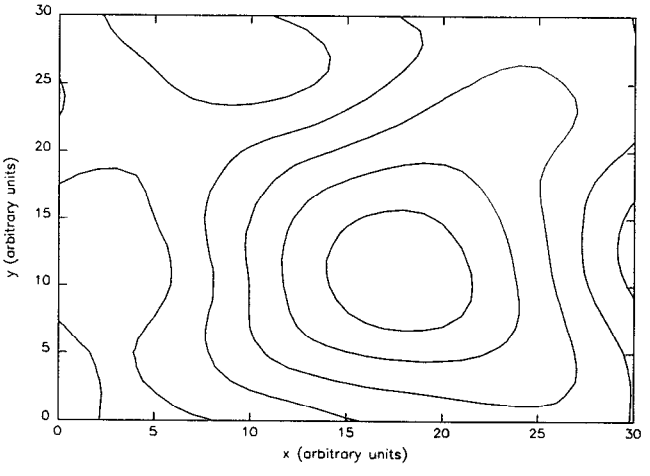

FIG. 8. Contours of constant density at the initial time in the relaxation of undriven/undamped turbulence. The peak at low k in the spectrum (Fig. 1) is evident in the large-scale structure of the contour plot.

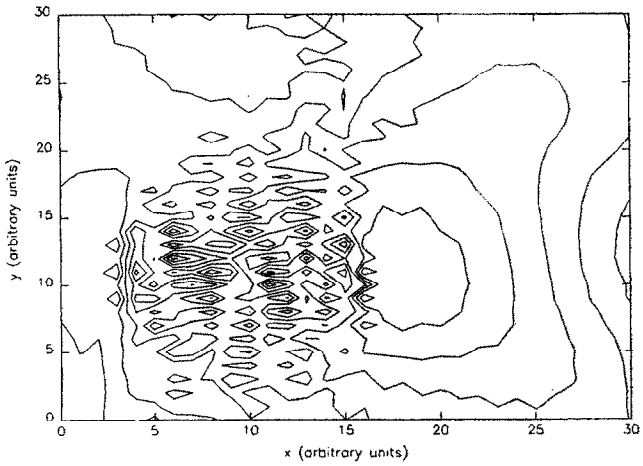

FIG. 9. Contours of constant density in the flow regime. Small-scale motion has been excited through the nonlinear transfer process with anisotropy due to the effectiveness of nonlocal transfer in the k_y direction.

tures, consistent with a spectrum peak at low k. As the spectrum evolves through the flow regime (excitation in the high k_y modes is growing rapidly) the anisotropy in the transfer manifests itself in an anisotropy in the isodensity contours. Small-scale structures appear in the k_y direction while few appear in the k_x direction. This can be easily misinterpreted as stretching in the k_x direction, but it should be remembered that the system is evolving by energy transfer from large-scale to small-scale structures. Hence, it is not stretching, but rather a breakup of the structure in the k_y direction that is occurring. In the sloshing regime, the contours relax to an approximately isotropic configuration, consistent with the isotropic equipartitioned equilibrium spectrum.

Transfer during the sloshing regime tends to be dominantly nonlocal in both the k_x and k_y directions. This is understandable because the mechanism that keeps the transfer local in k_x is suppressed in the sloshing regime. This mechanism is generally responsible for the locality of transfer in most systems, and stems from the amplitude dependence of

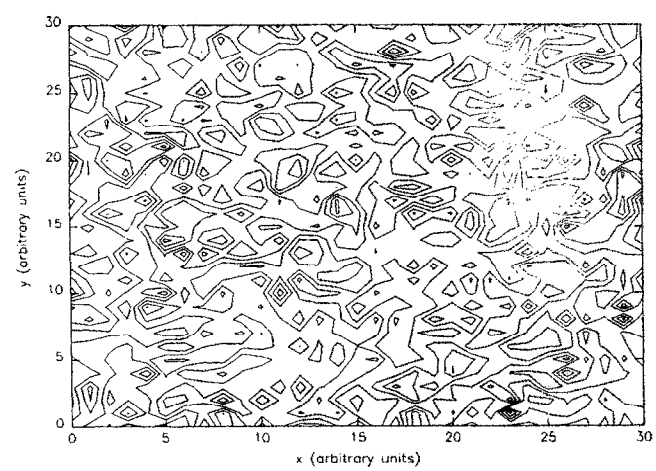

FIG. 10. Contours of constant density in the sloshing regime (see Fig. 3). Sloshing has isotropized the contours.

the transfer coupled with the fact that the amplitude distribution generally falls off with higher k. If the spectrum decays as $n \sim n_0 k^{-\alpha}$, then the transfer coupling between modes k and $k' > k$ goes as $T_k \sim n_k^2 n_{k'}^2 \sim n_0^4 k^{-2\alpha}(k'-k)^{-2\alpha}$ [using the closure representation, Eq. (2)]. Clearly, for $\alpha > 0$, transfer to neighboring modes $k' \gtrsim k$ is strongly favored over transfer to distant modes ($k' \gg k$). However, when the spectrum becomes nearly flat and $\alpha \approx 0$ (as in the case at the end of the flow regime), all modes have equal amplitude and the ratio of nonlocal to local transfer must increase.

This notion suggests that the strong nonlocal transfer in k_y exhibited in Fig. 6 should be suppressed if the initial spectrum is made sufficiently steep. Indeed, when the initial spectrum slope exceeds k^{-3}, nonlocal transfer is suppressed. In this case, transfer is local, producing a slow relaxation of the spectrum. Once the spectrum has relaxed to the k^{-3} slope, nonlocal transfer quickly begins and relaxation proceeds to the equilibrium spectrum at a much increased rate.

The dominance of nonlocal transfer over local transfer, as evidenced in Fig. 6, is strongly incompatible with the notion of a self-similar cascade that underlies the Kolmogorov-type spectrum [Eqs. (12) and (13)]. A similarity range cannot exist, at least in the k_y direction, as energy is transferred out of a mode and across the entire spectrum range in one correlation time. Indeed, the spectrum of steady state turbulence with driven modes at extremely low k, an intermediate inertial range over most of the spectrum, and a hyperviscosity at the highest wave numbers, bears no resemblance to the similarity range stationary spectrum of Eq. (13). Figure 11 reveals the stationary spectrum to be nearly flat with slight peaking at low k and strong quenching of the amplitudes in the dissipation range. While the inertial range is of limited extent in this spectrum (approximately one decade), the flatness is a robust feature independent of the strength of driving and the saturated turbulence level. Moreover, theoretical work based on the solution of a two-point equation likewise indicates that a flattening of the spectrum occurs as a result of the nonlocal transfer of the $E \times B$ nonlinearity.[16] Because the similarity range stationary spectrum differs so markedly from the numerical spectrum of stationary driven/damped turbulence, it is important to determine the direction of energy transfer in situations with spectra like that of Fig. 11. The transfer associated with the spectrum of Fig. 11 is found to be directed to large k, as would be expected from the configuration of sources and sinks. Moreover, the transfer from an initially flat spectrum in the undriven undamped case is also toward high k, producing a transfer rate history similar to that of Fig. 4, but with reduced magnitude. In this situation, nonlocal transfer proceeds in both directions whereas local transfer is directed to high k_y. Consequently, the spectrum develops a slight peak in k_y, and a sloshing regime ensues.

It is valid to ask whether the anisotropy in the transfer and the dominantly nonlocal transfer in the k_y direction are artifacts of the size of the k space. While it is not possible to say definitively that it is not an artifact, all evidence suggests that it is real. The wave number space has been varied from

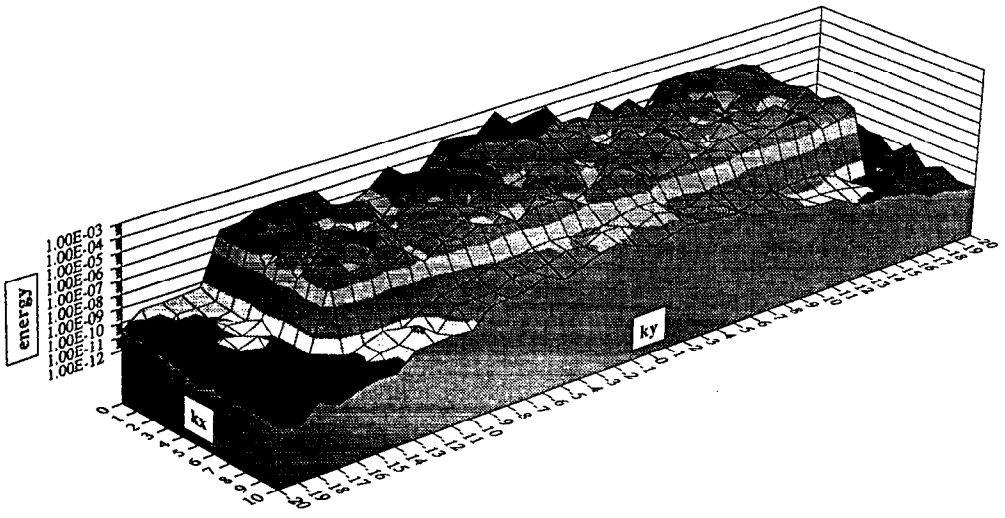

FIG. 11. Spectrum of turbulence driven at long wavelength and damped by a hyperviscosity at short wavelength with an inertial range in the intermediate modes. The spectrum is only slightly peaked in the inertial range, a result that differs markedly from the similarity range stationary spectrum [Eq. (9)]. The flatness of the spectrum is a result of the nonlocal transfer.

13×13 modes to 41×41 modes with the nonlocal and anisotropic features becoming more pronounced in the case of a larger k space, rather than the contrary. Furthermore, both the nonlocality and anisotropy are corroborated by the structure of the one-point closure equations and, to a lesser degree, the nonlinearity itself.

V. CONCLUSIONS

A numerical study of dissipative trapped ion convective cell turbulence has been described. This study is based on the spectral solution of the Kadomtsev–Pogutse equation. The primary focus has been on basic physics issues associated with the transfer dynamics of the dominant nonlinearity for long wavelength fluid plasma turbulence, the $E \times B$ nonlinearity. The principal results concern the equilibrium spectrum and its relation to statistical mechanics predictions, the direction of energy transfer in k space, and the nonlocality and anisotropy of the transfer process.

Finite-amplitude turbulence evolving in the absence of driving and damping has been found to undergo a relaxation in which spectra initially peaked at low k evolve to a flat, equipartitioned, and isotropic spectrum. The time-asymptotic spectrum is in good agreement with the predictions of equilibrium statistical mechanics and validates the assertion underlying the statistical mechanics calculation that the sole invariant constraining the dynamics of spectral transfer is the energy. The observed time-asymptotic spectrum also validates the statistical mechanics prediction that for a driven steady state with a spectrum peaked at low k, spectral energy flow will proceed from long to short wavelengths. The agreement with statistical mechanics is remarkable in that the analysis takes no account of a pronounced anisotropy in the nonlinearity and nonlinear transfer rate.

The transfer of energy occurring during the relaxation from a spectrum peaked at long wavelength to the equilibrium is measured to be in the direction of high k. Energy transfer occurs throughout the relaxation phase, with net time average transfer becoming zero when the equilibrium configuration is reached. A monotonically increasing enstrophy coincides with the phase of spectrum relaxation and net energy transfer to short wavelength. Enstrophy production is zero thereafter. With respect to its invariant properties and gross energy flow characteristics, it is clear that dissipative trapped ion convective cell turbulence is closer to 3-D Navier–Stokes turbulence than to its 2-D counterpart of Hasegawa–Mima drift wave turbulence. On the other hand, long wavelength drift wave turbulence (e.g., trapped electron mode turbulence) is closely related to the present model.[13]

On closer inspection, details of the energy transfer are found to deviate dramatically from the self-similar cascade, which represents the conventional wisdom for Navier–Stokes turbulence and inertial ranges in general. In particular, a robust and efficient nonlocal energy transfer process is observed that is capable of carrying energy from a low k mode to the other extreme of the spectrum in a correlation time. In the k_y direction this process dominates local cascading, except when the spectrum is sufficiently steep. Transfer in the k_x direction is divided equally between local and nonlocal components, implying a strong anisotropy in the transfer process. Nonlocal transfer violates the self-similarity hypothesis of Kolmogorov. Indeed, the inertial range spectrum in a driven/damped steady state is found to differ markedly from the Kolmogorov prediction.

The existence of a direct transfer of energy corroborates a key assertion of Ref. 4 and confirms the real possibility that dissipative convective cell turbulence plays a significant role in core fluctuation activity in hot tokamak discharges. Clearly, further work is needed, particularly is studying the transfer at smaller scales where the polarization drift nonlinearity becomes important and coupling to other short wavelength fluctuations becomes possible. The effect of the nonlocality of transfer on spectra, spatial transport, and other descriptive measures of turbulence also represents an issue requiring additional work.

ACKNOWLEDGMENTS

Useful conversations with G. G. Craddock and H. Biglari are acknowledged. P. H. D. acknowledges support from an Alfred P. Sloan Foundation Research Fellowship and a

National Science Foundation Presidential Young Investigator Award.

This work was supported by U.S. Department of Energy Contract No. DE-FG02-89ER-53291 and No. DE-FG03-88ER-53275.

[1] R. Saison, H. K. Wimmel, and F. Sardei, Plasma Phys. **20**, 1 (1978).
[2] H. Eubank, R. Goldston, V. Arunasalam, M. Bitter, K. Bol, D. Boyd, N. Bretz, J. P. Bussac, S. Cohen, P. Colestock, S. Davis, D. Dimock, H. Dylla, P. Efthimion, L. Grisham, R. Hawryluk, K. Hill, E. Hinnov, J. Hosea, H. Hsuan, D. Johnson, G. Martin, S. Medley, E. Meservey, N. Sauthoff, G. Schilling, J. Schivell, G. Schmidt, F. Stauffer, L. Stewart, W. Stodiek, R. Stooksberry, J. Strachan, S. Suckewer, H. Takahashi, G. Tait, M. Ulrickson, S. von Goeler, and M. Yamada, *Plasma Physics and Controlled Nuclear Fusion Research, 1978* (International Atomic Energy Agency, Vienna, 1979), Vol. 1, p. 167.
[3] W. Horton, D. I. Choi, P. W. Terry, and D. Biskamp, Phys. Fluids **23**, 590 (1980).
[4] H. Biglari, P. H. Diamond, and P. W. Terry, Phys. Rev. Lett. **60**, 200 (1988).
[5] P. H. Diamond and H. Biglari, Phys. Rev. Lett. **65**, 2865 (1990).
[6] R. J. Fonck, S. F. Paul, D. R. Roberts, Y. J. Kim, N. Bretz, D. Johnson, R. Nazikian, and G. Taylor, *18th European Conference of Controlled Fusion and Plasma Physics* (European Physical Society, Berlin, 1991), Vol. 15C, Part I, p. I-269.
[7] P. Cripwell and A. E. Costley, *18th European Conference of Controlled Fusion and Plasma Physics* (European Physical Society, Berlin, 1991), Vol. 15C, Part I, p. I-17.
[8] R. H. Kraichnan, J. Fluid Mech. **67**, 155 (1975).
[9] S. A. Orszag, in *Fluid Dynamics: Les Houches*, edited by R. Balin and J.-L. Peube (Gordon and Breach, New York, 1973), p. 235.
[10] F. Y. Gang, B. D. Scott, and P. H. Diamond, Phys. Fluids B **1**, 1331 (1989).
[11] G. G. Craddock, P. H. Diamond, and P. W. Terry, Phys. Fluids B **3**, 304 (1991).
[12] A. Hasegawa and K. Mima, Phys. Rev. Lett. **39**, 205 (1977).
[13] P. W. Terry and W. Horton, Phys. Fluids **25**, 491 (1982).
[14] G. G. Craddock (private communication).
[15] P. W. Terry and P. H. Diamond, Phys. Fluids **28**, 1419 (1985).
[16] P. W. Terry and P. H. Diamond, Bull. Am. Phys. Soc. **36**, 2346 (1991).